

Defect generation during solidification of aluminium foams

M. Mukherjee^{1,2,*}, F. Garcia-Moreno^{1,2}, J. Banhart^{1,2}

¹Helmholtz-Zentrum Berlin, Hahn-Meitner-Platz, 14109 Berlin, Germany

²Technische Universität Berlin, Hardenbergstrasse 36, 10623 Berlin, Germany

The reason for the frequent occurrence of cell wall defects in metal foams was investigated.

Aluminium foams often expand during solidification, which is referred as solidification expansion (SE). The effect of SE on the structure of aluminium foams was studied in-situ by X-ray radiography, and ex-situ by X-ray tomography. A direct correlation between the magnitude of SE and the number of cell wall ruptures during SE and finally the number of defects in the solidified foams was found.

Keywords: Metal foam; Aluminium; Solidification expansion; Rupture; Defect

* Corresponding author: M. Mukherjee. Address: Helmholtz-Zentrum Berlin, Hahn-Meitner-Platz, 14109 Berlin, Germany. Phone: +49 30 8062 2820. Fax: +49 30 8062 3059.

E-mail: manas.mukherjee@gmail.com

Solidification of metallic foams is an inevitable step in the manufacture of these materials since gas is generated in the liquid state while a solid cellular material has to be made. The solidification step is very complex since at falling temperatures the properties of the metal, the pressure difference between the interior and the surroundings and the kinetics of gas release from the blowing agent change. It has been found that in many cases the foamed metal re-expands during solidification [1]. This effect is referred as *solidification expansion* or SE. It is mainly caused by

continued gas evolution from the blowing agent concomitant with reduced gas losses by out-diffusion and the shrinkage of the gas in the cells due to the temperature drop [2,3].

Often metal foams are prepared inside a closed metallic mould which allows for making shaped foam parts. Filling moulds can be difficult since the foam tends to collapse and to recede from the mould walls after mould filling due to the higher temperature of the mould. SE is seen as a potential strategy to fill moulds completely. One could tailor the cooling rate such that the foam re-expands shortly before complete solidification [2,3]. However, if SE is too high it could lead to adverse effects on foam morphology.

In this article, we study SE in two Al-based alloys cooled at different rates. It was observed that a high SE induces cell wall rupture which eventually generates defects in the foam. It is well-known that foams blown by a gas releasing agent often contain many structural defects such as missing or broken cells, partially coupled or elliptical cells. Such defects can cause a drastic deterioration of the mechanical properties [4–7]. The origin of some of these defects could be explained by our findings.

Foams were produced by the powder compact route. Aluminium (Alpoco, 99.7 wt.% pure), silicon (Wacker Chemie, 99.5 wt.% pure) and copper (Chempur, 99.5 wt.% pure) metal powders and powdered TiH₂ (Chemetall, Grade N, 98.8 wt.% pure) were used to prepare foamable precursors. The TiH₂ powder that served as blowing agent was heat-treated at 480 °C for 180 minutes in air prior to use in order to shift the hydrogen release range to higher temperatures. To prepare precursors, 30 g of metal powders were mixed with 0.5 wt.% of heat-treated TiH₂ powder for 15 min. The powder blend was subjected to uni-axial hot compaction for 5 min at 400 °C applying a pressure of 300 MPa. Cylindrical tablets (36 mm diameter, ~11 mm thick) were obtained. Samples measuring 10 × 10 × 4 mm³ were cut out of these tablets, ensuring that the compaction direction that later defines the foaming direction was along the 4 mm long side of the sample. AlSi6Cu4 and AlSi7 alloys were investigated in this study.

Foaming was carried out in an X-ray transparent furnace based on two halogen lamps equipped with infrared reflectors and providing in total 2×150 W heating power. Foaming was performed inside a steel tube (25.5×25.5 mm² inner cross section, 2 mm wall thickness) that was 28 mm long along the direction of the X-ray beam. The open ends of the tube were covered with aluminium foils (thickness 30 μ m) to minimize heat losses by convection. The steel tube was placed on a ceramic plate to further minimize heat losses. Although inserting a thermocouple far enough into the small foaming specimens would ensure a reliable temperature measurement, this would affect the stability and expansion of the foams too much and also interfere with the X-ray imaging. Therefore, a thermocouple was inserted only 0.5 mm deep into the foam from below through a hole in the steel tube. Precursors were foamed by heating them to above their melting point. The foaming temperature – as read at the surface of the sample – was 600 °C for both alloys. This corresponds to a temperature of about 620 °C at the centre of the sample as determined by separate calibration tests. Unless otherwise indicated, the temperatures reported in this article were measured at the bottom surface.

Heating from room temperature (~ 30 °C) up to 600 °C was performed with a heating rate of 2–3 K/s, after which the temperature was held at 600 °C for a given period which is referred here as *holding time*. After holding, the foam was solidified either by *natural cooling* – performed by simply turning off the power supply of the lamps – or by *slow cooling* – achieved by reducing the power supply of the lamps from 300 W to a lower value. All the measurements were repeated three times for each experimental condition.

Foaming was continuously monitored *in-situ* by using an X-ray radioscopy set-up comprising a micro-focus X-ray source and a panel detector, for details see Ref. [8]. The X-ray source was used with 5 μ m spot size at 100 kV voltage and 100 μ A current. X-ray-projected images of the foam were acquired every two seconds. Projected foam area and number of cell wall rupture events as a function of time were determined by image analysis using the dedicated software ‘AXIM’ [8]. An expansion curve is then given by the projected area of the sample for the entire

foaming process. For the detection of rupture, consecutive image pairs are compared. All the pixels for which the grey levels change by more than a given threshold value are identified. If such pixels form a cluster that is larger than another threshold value and if that cluster is separated from other already identified clusters by a given minimum distance, it is considered a *rupture event*. More details of the analysis are given in Refs. [9,10]. The threshold parameters were chosen such that micropore ruptures and very small movements were not taken into account. Moreover, other artefacts could be avoided, e.g. that the rupture of a large cell appeared as several individual rupture events.

X-ray tomography of the solidified foams was performed using the same X-ray set-up but rotating the foam by 360° in steps of 1° while acquiring images after each step. Three-dimensional reconstruction of the data was performed using the commercial software ‘Octopus’. After reconstruction, the commercial software ‘VGStudioMax 1.2.1’ was used to extract 2D sections of the foam.

The foaming behaviour of AlSi6Cu4 and AlSi7 alloys is shown in Fig. 1a and 1b. Slow cooling was performed by reducing the power supply of the lamps from 300 W to 180 W (151 W) for AlSi6Cu4 (AlSi7). SE can be observed in all the measurements. In these alloys, SE takes place in two stages: SE1, which is observed during primary α -aluminium solidification; and SE2, which is observed during Al-Si eutectic solidification [2,3]. In this article we only focus on SE1, the reason for which will be discussed later on. The cooling rates reported in this article represent the average cooling rate during SE1. In AlSi6Cu4 foams, SE1 is 4.4% or 29.9% for natural or slow cooling, respectively, while in AlSi7 the corresponding values for SE1 are 17.9% (46%) for natural (slow) cooling. Two other measurements for each condition produced similar results as shown in Fig. 2.

The number of rupture events was determined for both the alloys solidified at the cooling rates shown in Fig. 1. Additionally, a further cooling rate of 0.82 K/s was applied to AlSi7 foams, achieved by reducing the power supply to 136 W. We report only those ruptures that occurred after the onset of SE. Most rupture events are found in the stage of SE1 with only few observed during

SE2. The number of ruptures during SE1 is shown as a function of the magnitude of SE1 in Fig. 2. Each data point is an average of three measurements; the error bars represent standard deviation. The trend in Fig. 2 suggests that the number of ruptures is intimately related with SE1.

Fig. 3 shows various stages of a particular rupture event that occurred during SE1. The foam was produced by first holding for 600 s and then solidifying with the low cooling rate of 0.28 K/s. SE1 in this foam is 12%. The rupture depicted in Fig. 3 initiates by first stretching and thus thinning the central part of the cell wall as visible in the image taken at $t=1158$ s. The length of the cell wall, represented by the broken arrow in the $t=1148$ s image, increases by 8% in the 10 s after, while the height and area of the entire foam increase only by 1% and 2.7%, respectively. At $t=1160$ s, the central part breaks and subsequently the ruptured ends separate as seen in the $t=1166$ s image. At $t=1148$ s, the temperature has reached about 575 °C, which is the real (not surface) temperature of the sample, and the rupture event has completed within a temperature drop of 5 K.

The structure of the solidified foams was visualized by means of X-ray tomography. A representative macrostructure of the foams is shown in Fig. 4. After natural cooling, the cell walls of the foams are free of defects except for small defects as seen for AlSi7 foam in Fig. 4c. In contrast, most of the cell walls are broken in the slowly cooled foams as shown in Fig. 4b and 4d.

Longer solidification time increases the accumulated hydrogen production from the blowing agent during solidification and causes the observed increase in SE1 [2,3]. This SE1 varies significantly with cooling rate as shown in Figs. 1 and 2. On the other hand, SE2 remains at a nearly constant low $\approx 2\%$ level for all cooling rates [2,3]. Clearly, the influence of SE1 on foams varies from one cooling rate to another, whereas SE2 must have the same influence (if any) for all cooling rates. Hence, the main focus of this study was to explore the consequence of different SE1.

As foam grows, its cell walls become thinner due to stretching. Eventually, after reaching a critical thickness, cell wall rupture leads to coalescence of two cells. Therefore, it is generally believed that expansion of foams is always associated with coalescence of cells, a phenomenon known as ‘growth coalescence’ [11,12]. Similarly, cell walls are expected to rupture whenever a

foam expands during solidification. Hence, the number of ruptures increases with increasing SE1 as shown in Fig. 2.

Note that even if SE1 is small a cell wall can still rupture due to a high local SE1 as observed in Fig. 3. Since the distribution of TiH_2 in the foaming samples is statistical, the concentration of TiH_2 in some parts of the foam is higher than in other parts. As a result, the production of hydrogen in some parts is elevated, resulting in a larger local SE1 than the global value.

Partially broken cell walls in solid foams would not be observed if rupture took place in the fully liquid state. This is because after rupture the entire melt contained in that cell wall is redistributed into the surrounding structure and the geometry is readjusted to a new equilibrium structure leaving no trace of the ruptured cell wall. The process is completed within a period of 300–1000 μs [13,14]. Such a fast process infers that rupture is dominated by surface tensional forces and not by the viscosity of the melt [13].

During solidification the viscosity of the melt increases continuously with the volume fraction of solid metal. In Fig. 3, rupture initiates at 575 °C. At that temperature the melt contains about 40% of solidified phase [15]. Consequently, the viscosity is at least two orders of magnitude higher than the viscosity of the fully liquid metal [16]. This implies that during solidification rupture is increasingly dominated by the viscosity of the semi-solid melt, which can significantly slow down the process [11]. This even enables us to detect the moment of rupture in the present study where the image acquisition rate was only 0.5 Hz. Under these conditions, the foam has solidified before the melt of the rupturing cell wall has been redistributed. Thus the frozen rupture event remained as defect in the solid foam.

It has been shown in Fig. 2 that with decreasing cooling rate the number of ruptures during SE1 increases. The broken ends of some ruptured cell walls may remain as defect in solid foam as shown in Fig. 3. It is unlikely that all ruptures during SE1 end up as defects because at the beginning of SE1 the melt contains just about 25% of solid phase [3], which is most likely

insufficient to slow down the redistribution of the melt of ruptured cell wall significantly. At later stages of SE1, the solid content increases sharply and therefore the viscosity of the melt is sufficient to arrest redistribution of the melt, thereby generating the observed defects. Therefore, it is anticipated that the number of defects in slowly cooled foams should be higher than that in naturally cooled foams. Fig. 4 justifies this hypothesis. For AlSi7 foam, even for natural cooling defects are observed because of the high SE1 value there as shown in Figs. 1b and 2. The number of defects in slowly cooled foams is so high that all the cells in the entire cross section are interconnected in Fig. 4b and 4d.

The defects shown in Fig. 4 are identical to the most frequently observed defects in metal foams produced by blowing with TiH_2 [4–7]. Interconnectivity as demonstrated in Figs. 4b and 4d has also been reported for ‘Alporas’ and ‘Alulight’ foams in Ref. [17]. Therefore, it is very likely that the defects usually observed in foams blown by TiH_2 are caused by SE.

SE1 in this study was deliberately increased by slowing down the cooling process. The cooling in the manufacture of large foam parts will be inherently slow due to the low thermal conductivity of foams. Therefore, if the blowing agent is still active during solidification of a large foam, defect generation due to SE cannot be avoided. We propose the following strategies to reduce defects in foam structure – 1) increase in cooling rate by, for instance, forced air cooling, 2) increase in holding time and 3) combination of both.

In summary, we could identify one of the reasons which lead to defects in aluminium alloy foams. The mechanism is linked to the phenomenon of expansion during solidification, which is referred as SE. The magnitude of SE increases when the cooling rate decreases. Consequently, the number of ruptures associated with SE also increases with a decrease in cooling rate. Cell wall rupture during solidification slows down because of the high viscosity of the semi-solid melt. As a result, in some cases, the broken ends of the ruptured cell are present as defects in the solid foam. Slowly solidified foams contain more defects than foams solidified at a high rate because of a higher value of SE in the former case.

- [1] M. Mukherjee, F. Garcia-Moreno, J. Banhart, *Trans. Indian. Inst. Met.* 60 (2007) 133.
- [2] Mukherjee M. Thesis, Technische Universität Berlin, 2009.
- [3] M. Mukherjee, F. Garcia-Moreno, J. Banhart, submitted to *Acta Mater.*
- [4] A-F. Bastawros, H. Bart-Smith, A.G. Evans, *J. Mech. Phys. Sol.* 48 (2000) 301.
- [5] A.E. Markaki, T.W. Clyne, *Acta Mater.* 49 (2001) 1677.
- [6] U. Ramamurty, A. Paul, *Acta Mater.* 52 (2004) 869.
- [7] I. Jeon, T. Asahina, *Acta Mater.* 53 (2005) 3415.
- [8] F. García Moreno, M. Fromme, J. Banhart, *Adv. Eng. Mater.* 6 (2004) 416.
- [9] F. Garcia-Moreno, M. Mukherjee, C. Jimenez, J. Banhart, *Trans. Indian. Inst. Met.* 62 (2009) 451.
- [10] F. Garcia-Moreno, E. Solórzano, J. Banhart, in preparation.
- [11] C. Körner, M. Arnold, R.F. Singer, *Mater. Sci. Eng. A*, 396 (2005) 28.
- [12] C. Körner, *Mater. Sci. Eng. A*, 495 (2008) 227.
- [13] F. García-Moreno, A. Rack, L. Helfen, T. Baumbach, S. Zabler, N. Babcsán, J. Banhart, T. Martin, C. Ponchut, M. Di Michiel, *App. Phys. Lett.* 92 (2008) 134104-1.
- [14] A. Rack, F. García-Moreno, T. Baumbach, J. Banhart, *J. Synchrotron Radiat.* 16 (2009) 432.
- [15] JMatPro, Sente Software Ltd. United Kingdom.
- [16] M.C. Flemings, *Met. Trans. A*, 22A (1991) 957.
- [17] E. Solórzano, M.A. Rodríguez-Pérez, J.A. de Saja, in: J. Hirsch, B. Skrotzki, G. Gottstein (Eds.), *Aluminium Alloys: Their Physical and Mechanical Properties*, Wiley-VCH, Weinheim, 2008, pp. 2200–2206.

Figure captions

Figure 1. Foaming behaviour of (a) AlSi6Cu4, holding time 200 s and (b) AlSi7, holding time 100 s. The beginning of solidification expansion (SE) in each curve is indicated. The cooling rates mentioned in the legend represent the average cooling rate during SE1. The period of SE1, t_{SE1} , is shown for the slowly cooled foams.

Figure 2. Accumulated number of cell wall rupture events in the entire foam during SE1, i.e. period t_{SE1} in Fig. 1, as a function of SE1. Holding time is 200 s for AlSi6Cu4 and 100 s for AlSi7. The number beside each data point is the respective cooling rate in K/s.

Figure 3. X-ray image sequence of different stages of rupture of a cell wall (indicated by arrow) during solidification of AlSi6Cu4 foam. Temperature drop at $t=1158$ s, 1160 s and 1166 s compared to the stage at $t=1148$ s is indicated in the lower left corner. The foam is solid at $t=1440$ s. The broken ends of the ruptured cell wall in the solid foam are marked by ellipses.

Figure 4. 2D slices of X-ray tomograms of AlSi6Cu4 (a and b) and AlSi7 (c and d) foams solidified with natural (a and c) and slow (b and d) cooling. These foams correspond to those shown in Fig. 1. Images represent approximately the central section of the foams along the foaming direction. Some broken cell walls are indicated by arrows. The broken lines in (b) and (d) indicate interconnection of cells.

Figure 1a and 1b
[Click here to download high resolution image](#)

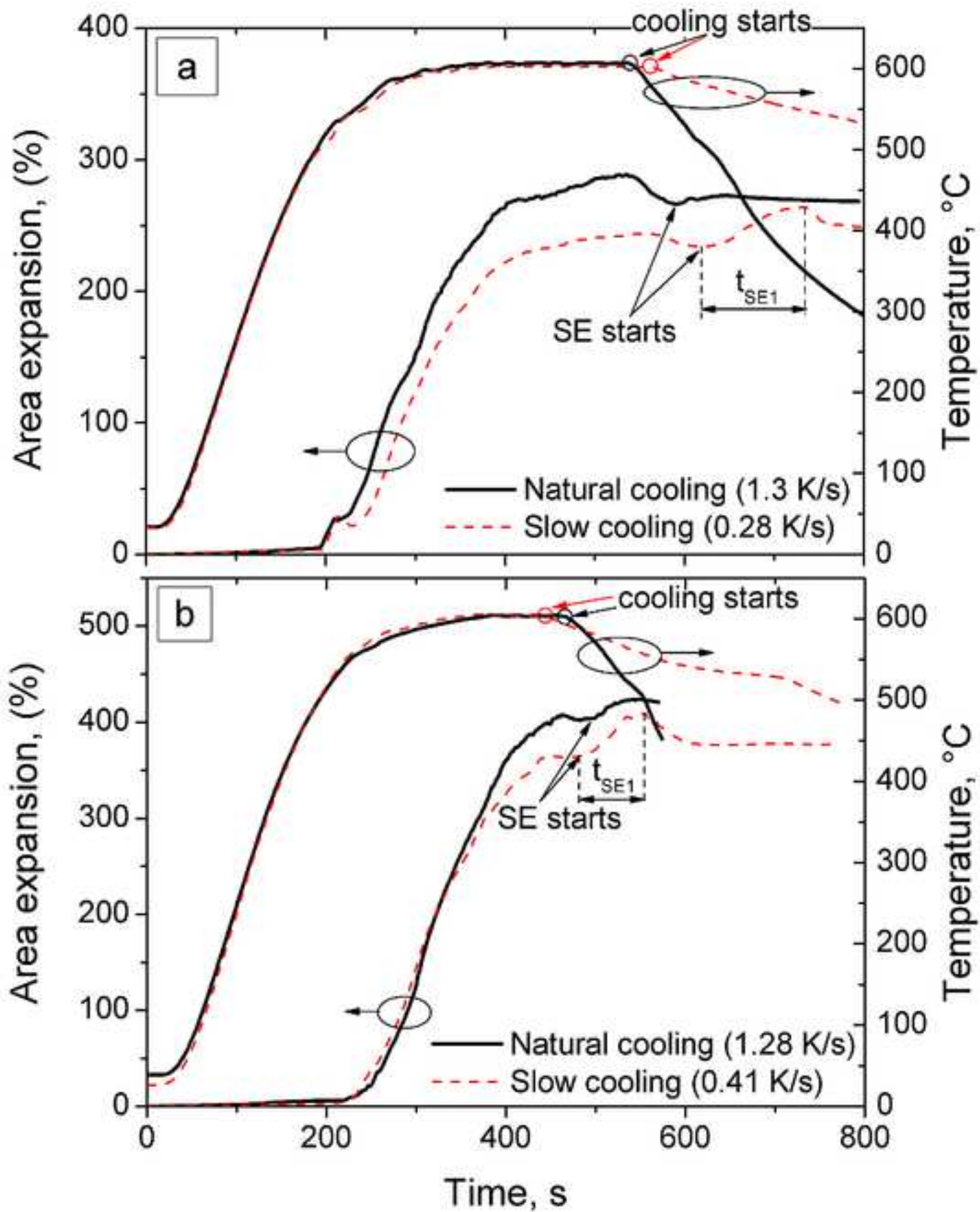


Figure 2
[Click here to download high resolution image](#)

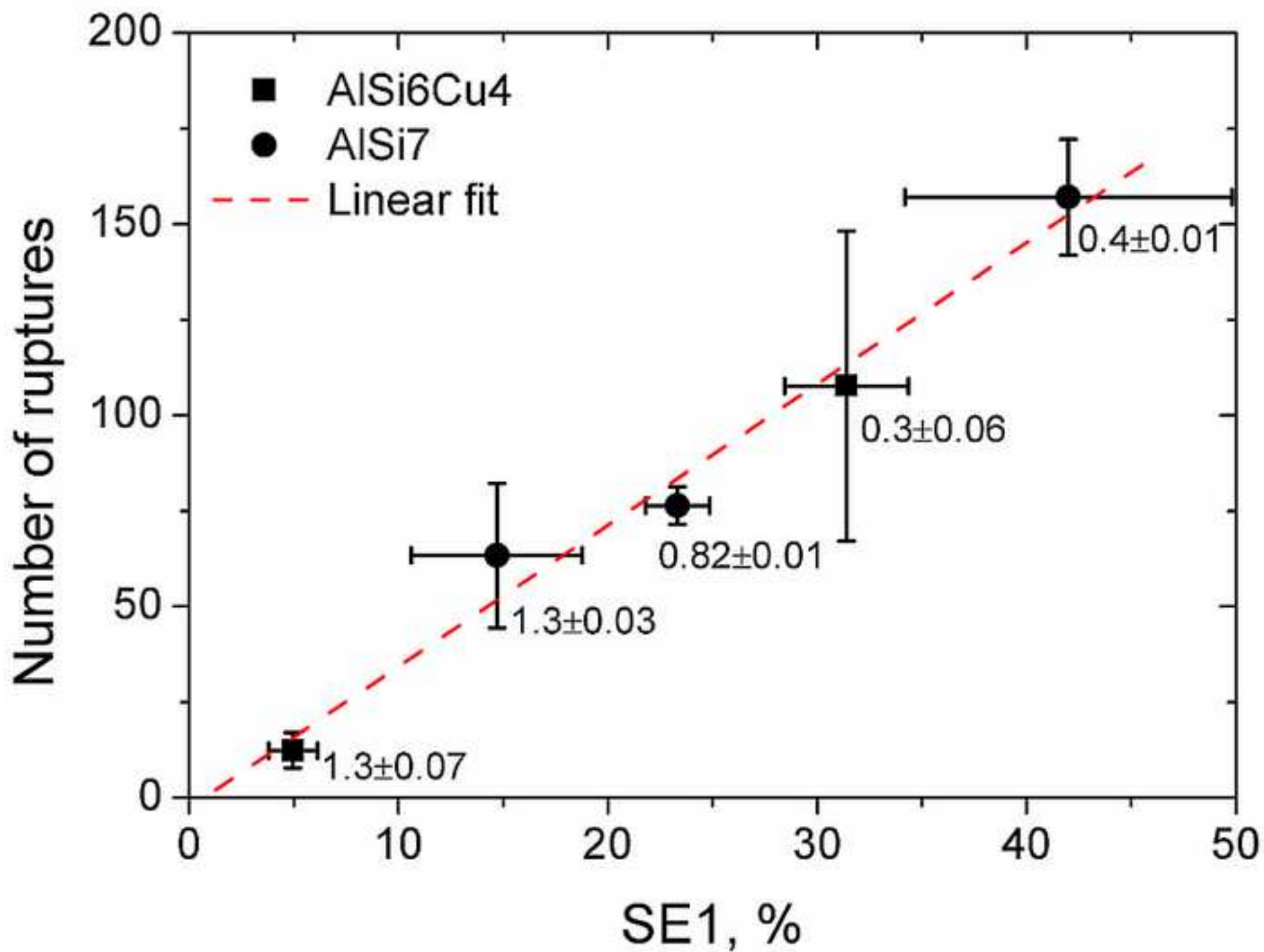


Figure 3
[Click here to download high resolution image](#)

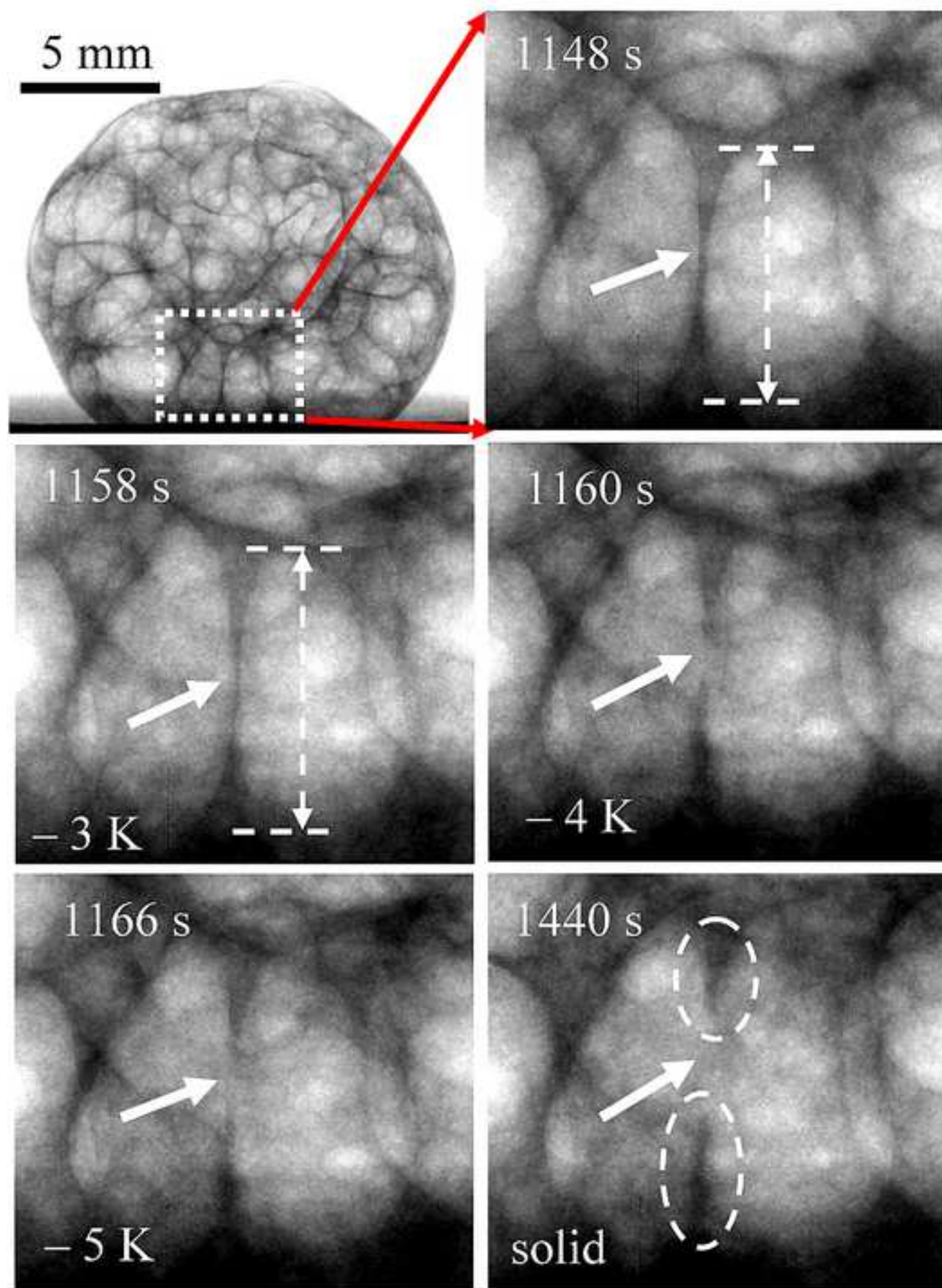


Figure 4
[Click here to download high resolution image](#)

